Nanotechnology **20** (2009) 325707 (5pp) doi:10.1088/0957-4484/20/32/325707

A carbon nanotube field emission cathode with high current density and long-term stability

Xiomara Calderón-Colón[1], Huaizhi Geng[2], Bo Gao[2], Lei An[3], Guohua Cao[3] and Otto Zhou[1,3]

[1] Curriculum in Applied Science and Engineering, University of North Carolina at Chapel Hill, Chapel Hill, NC 27599, USA
[2] Xintek, Incorporated, 7020 Kit Creek Road, Research Triangle Park, NC, USA
[3] Department of Physics and Astronomy, University of North Carolina at Chapel Hill, Chapel Hill, NC 27599, USA

Received 26 March 2009, in final form 10 June 2009
Published 21 July 2009
Online at stacks.iop.org/Nano/20/325707

Abstract
Carbon nanotube (CNT) field emitters are now being evaluated for a wide range of vacuum electronic applications. However, problems including short lifetime at high current density, instability under high voltage, poor emission uniformity, and pixel-to-pixel inconsistency are still major obstacles for device applications. We developed an electrophoretic process to fabricate composite CNT films with controlled nanotube orientation and surface density, and enhanced adhesion. The cathodes have significantly enhanced *macroscopic* field emission current density and long-term stability under high operating voltages. The application of this CNT electron source for high-resolution x-ray imaging is demonstrated.

(Some figures in this article are in colour only in the electronic version)

Because of their promising electron field emission characteristics [1] and potential for low-cost manufacturing, carbon nanotubes (CNTs) are now being investigated as 'cold-cathodes' for a wide range of applications. Prototype devices including field emission display (FED) [2], back light unit for liquid crystal display [3], x-ray source [4, 5], electron gun for electron microscope [6], and microwave amplifier [7, 8] have been demonstrated. Novel x-ray computed tomography (CT) systems for preclinical and clinical imaging using the CNT x-ray technology are also under development [9, 10]. The requirements for the CNT field emission cathodes vary significantly from device to device. FED typically uses a relatively low anode voltage (∼10 kV) and a low emission current density but requires up to millions of addressable pixels to perform consistency over a long period of time under poor vacuum conditions [1, 11]. X-ray generation requires extremely high current density in the order of 10^2–10^3 mA cm^{-2} and acceleration voltage ranging from 30 kV for mammography to over 180 kV for airport baggage inspection. High current density is also required by microwave tubes [8, 12].

Most of the published CNT field emission research so far has focused on FED. The behavior of the macroscopic CNT cathodes under high emission current and high voltage has not been adequately investigated except a few published studies with less than satisfactory results [8, 13, 14]. We have earlier reported ∼4 A cm^{-2} current density from SWNT films [13], from local point probe measurement in the diode mode without high voltage. No lifetime information was obtained at the high current density. In a separate study using a large area CNT cathode made by spraying, a high total current and high current density were observed in micro-second pulsed emission [14]. The cathode however failed within a few milliseconds due to evaporation of the CNTs under high field. By direct chemical vapor deposition growth of CNTs with controlled spacing using nanometer scale catalysts patterned e-beam lithography, Milne *et al* has successfully obtained 1 A cm^{-2} emission current density from a millimeter-size CNT cathode [8]. Long-term stability and high voltage stability of these cathodes however are unknown. Although an individual CNT can emit over 1 μA [15–17], obtaining high current from a *macroscopic* cathode is difficult [18]. Limited by the emitter non-uniformity and electrical screening effect the density of active emitters is typically low. This results in a high current from each active emitter even under a moderate extraction current density

which leads to failure of the nanotubes within a relatively short time. Adhesion of the CNTs to the substrate surface also plays a significant role in the emission stability, especially under high voltage. Removal of the CNTs under high potential is a common cause of arcing which is detrimental to vacuum electronic devices.

We have previously reported a liquid-phase room temperature electrophoretic deposition (EPD) method for fabrication of patterned CNT films [19]. Here we investigated the effects of morphological parameters on the field emission properties of *macroscopic* CNT films and showed that by optimizing the surface orientation and density of the CNTs and improving the adhesion, CNT cathodes with long-term stability under high current and high voltage conditions can be manufactured.

For cathode fabrication multi-wall CNTs with outer-shell diameters of 3–8 nm synthesized by the thermal CVD process were used as the staring material [20]. After purification, they were dispersed in alcohol together with $MgCl_2$ which serves as the charger. To improve the adhesion glass frits as a binders were added to the EPD ink [21]. Glass with printed Ag contact lines or metal plates was used as the substrates. The deposition procedure is similar to what has been described in our previous publication [19] and is illustrated in figure 1. Under a DC electrical field, the electrically charged CNTs and the binders were driven to and deposited onto the substrate surface to form a composite film composed of the CNTs dispersed in the binder matrix. The film thickness was controlled by the deposition time and the voltage applied. In this study, the CNT concentration, the deposition condition, and thickness of the photoresist were systematically varied.

The surface morphologies of the film formed were studied by optical microscope and SEM at different processing stages. Most of the materials were deposited into the exposed area on the conducting substrate although some were also found around the edges of the SU-8 photoresist, as shown by the optical images in figure 1. The bonding between the CNT composite film and the substrate was strong enough that most of the CNTs remained on the substrate surface after photoresist liftoff. SEM micrographs (figure 2) show that the CNTs were randomly oriented after EPD and after vacuum annealing at 10^{-6} Torr vacuum for one hour at 500 °C. The surface CNTs became vertically aligned with one ends embedded inside the matrix and the other ends protruding from the surface after the activation process—mechanically removal of a top surface layer of the composite film using an adhesive tape, as shown by cross-section SEM image in figure 2(c). This is the desired morphology for field enhancement and for adhesion. The protruding length of the CNTs is remarkably uniform considering the large length variation of the raw CNTs. After annealing, the composite film bonded strongly to the substrate surface and could not be removed by taping. This is drastically different from the typical CNT films directly grown by the chemical vapor deposition which have very weak interface bonding. A strong adhesion is achieved in these films because they are composites rather than bare CNTs and the protruding CNTs are partially embedded inside the matrix.

The density of these protruding CNTs can be controlled by the starting concentration of the CNTs in the EPD ink.

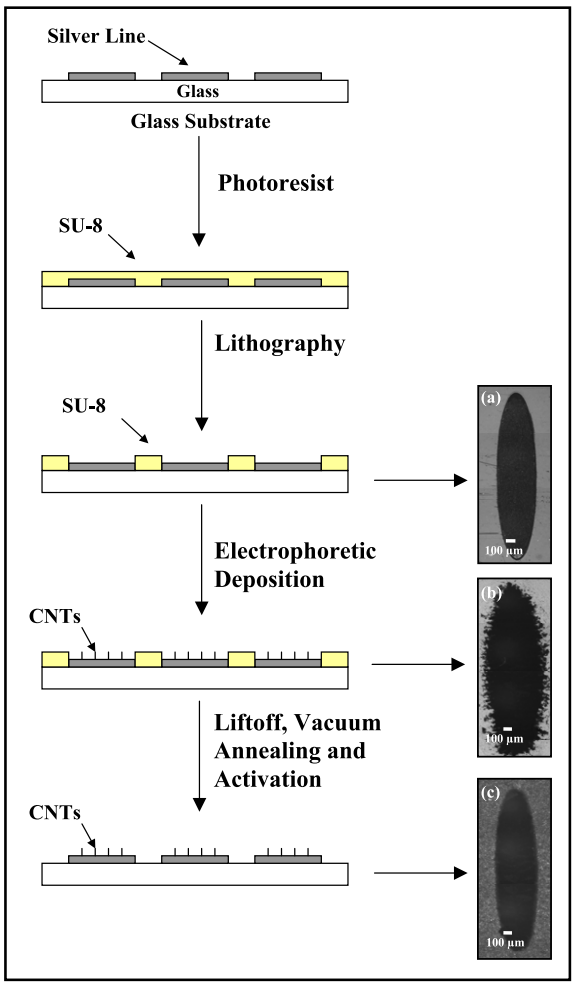

Figure 1. A scheme showing the procedure used to patterned deposition of CNT cathode by EPD. Optical microscope images showing an elliptical cathode after; (a) photolithography, (b) CNT deposition, and (c) liftoff with NMP and vacuum annealing.

A series of 4 cathodes were made using inks with increasing CNT concentration ($\times, 2\times, 4\times$, and $8\times$) while the other parameters were kept the same. Although the exact value is difficult to determine, cross-section SEM images (figures 2(d) and (e)) clearly showed the density of vertically aligned CNTs increases with increasing CNT concentration of the EPD ink. For the cathode shown in figure 2(d), the ratio between the height (L) of the protruding CNT and their average spacing (D) was estimated to be close to 1. The ratio is significantly smaller for the sample shown in figure 2(e) which was made using an EPD ink with $4\times$ higher the CNT concentration compared to the cathode shown in figure 2(d).

The film thickness depended on the deposition conditions used such as the current, deposition time, and voltage applied. For cathodes made under the same conditions, the average film thickness is 15 μm and consistent with less than 10% variation. Measurement by profilometer shows that the film was slightly thicker around the edge than in the center. The variation is about 5–10 μm over ~2000 μm distance. This is attributed to the electrical field concentration around the edge of the exposed metal contact line during EPD process which causes a high rate of CNT deposition. Edge effect

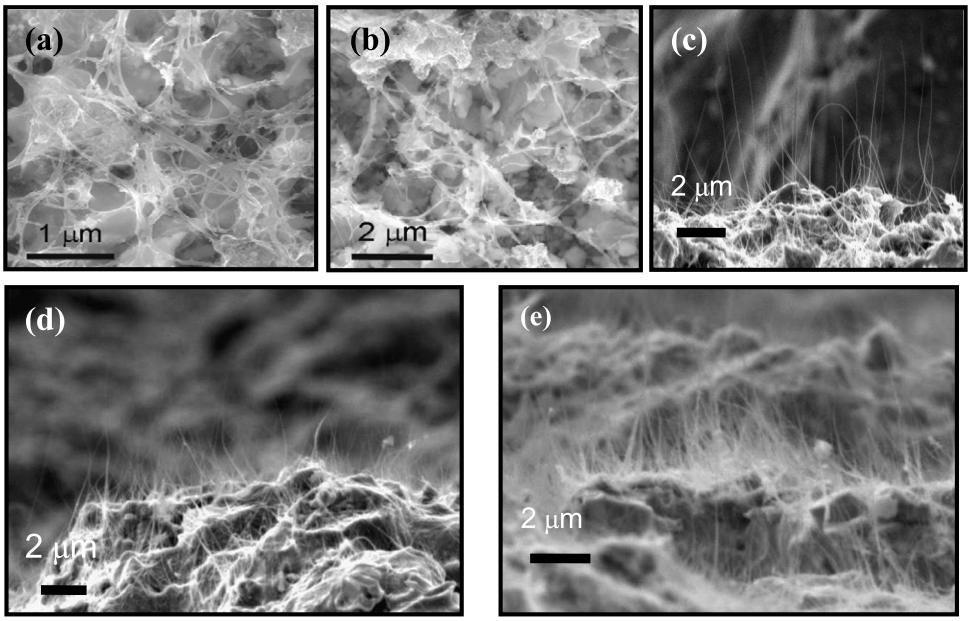

Figure 2. SEM images showing the top surface of the composite CNT film both: (a) before and (b) after vacuum annealing. The CNTs are randomly oriented on the surface. (c) Cross-sectional SEM image of the CNT cathode after the activation process. The surface CNTs are now vertically aligned in direction perpendicular to the substrate surface. Cross-sectional SEM images of two cathodes fabricated under the same conditions except different CNT concentrations in the EPD inks. Cathode shown in (e) was made using an ink with 4× the CNT concentration than the cathode shown in (d).

is known to cause preferential emission from the edges [22] which reduces the overall performance. This was partially mitigated by increasing the thickness of the photoresist. The thickness variation was reduced by 40% when the thickness of the photoresist was increased from 10 to 100 μm.

To evaluate the electron field emission properties of the CNT cathodes fabricated, a large group of samples were fabricated. For convenience of evaluation and comparison the cathodes fabricated have an elliptical geometry. The emission properties, as indicated by the electrical field required for a given emission current, were found to be primarily determined by the surface density of the vertically aligned CNTs. For the group of samples made with increasing surface CNT densities, the cathode with the D/L ratio of $\sim$1 showed the lowest extraction electrical field for a given current density. This is consistent with the known electrical screening effect for multiple emitters.

For cathodes fabricated with optimized surface CNT density a stable emission current density over 1500 mA cm^{-2} was readily obtained. Figure 3(a) plots the experimentally measured emission current densities versus the applied electrical fields for three different size cathodes. The results also indicate that there is still room for improvement in terms of the sample non-uniformity. At the same applied electrical field, the smaller the cathode area, the higher the current density achieved. For example, the smallest cathode (0.08 mm^2) reached a current density of over 1400 mA cm^{-2} while the large one (0.92 mm^2) generated $\sim$400 mA cm^{-2} density at the same applied field of 8.5 V μm^{-1}. This is attributed to the edge effect observed in the profilometer measurement. Cathodes with similar CNT surface density but different deposition time and film thickness have similar emission properties. Figure 3(b) shows the electrical fields required to reach 1 mA (108 mA cm^{-2}) and 6 mA (650 mA cm^{-2}) measured from a group of 12 cathodes. The small sample to sample variation demonstrates the reliability of this fabrication process.

The cathodes were further evaluated under high anode voltage in the triode mode using a micro-focus field emission x-ray tube [5] illustrated in figure 4(a) inset. After the initial conditioning process, the CNT cathode and the field emission x-ray were operated stably at the anode voltage of 50 kV, the highest voltage allowed by the feed-through. In separate studies in different x-ray systems, stable operations have been achieved at 140 kV. As shown in figure 4(a), a stable cathode current of 3 mA (325 mA cm^{-2}) was readily obtained at the gate voltage (V_g) of $\sim$1800 V from a 0.50 mm × 2.35 mm elliptical CNT cathode. About 60% of the cathode current reached x-ray anode with the rest leaked through the gate and focusing electrodes. For comparison, the result from the same cathode measured in the diode mode was also plotted in the same figure. The difference in the extraction field is attributed to the field non-uniformity caused by the metal mesh gate electrode (Tungsten gauze, 100 mesh woven) used in the x-ray tube.

The long-term emission stability was evaluated by measuring the variation of the applied V_g needed to maintain a constant 3 mA cathode current, which is close to the maximum current allowed under the present conditions. Due to limitations of the anode heat dissipation the maximum power P_{max} (in watts) of a fixed anode micro-focus x-ray tube can be estimated as $P_{max} \approx 1.4(X_{f,FWHM})^{0.88}$ [23], where $X_{f,FWHM}$ is the focal spot size in microns. For the 0.50 mm × 2.35 mm elliptical cathode with an effective focal spot size of $\sim$100 μm × 100 μm [9] P_{max} is $\sim$80 W or $\sim$3 mA cathode current (with $\sim$60% transmission rate) at 40 kV anode

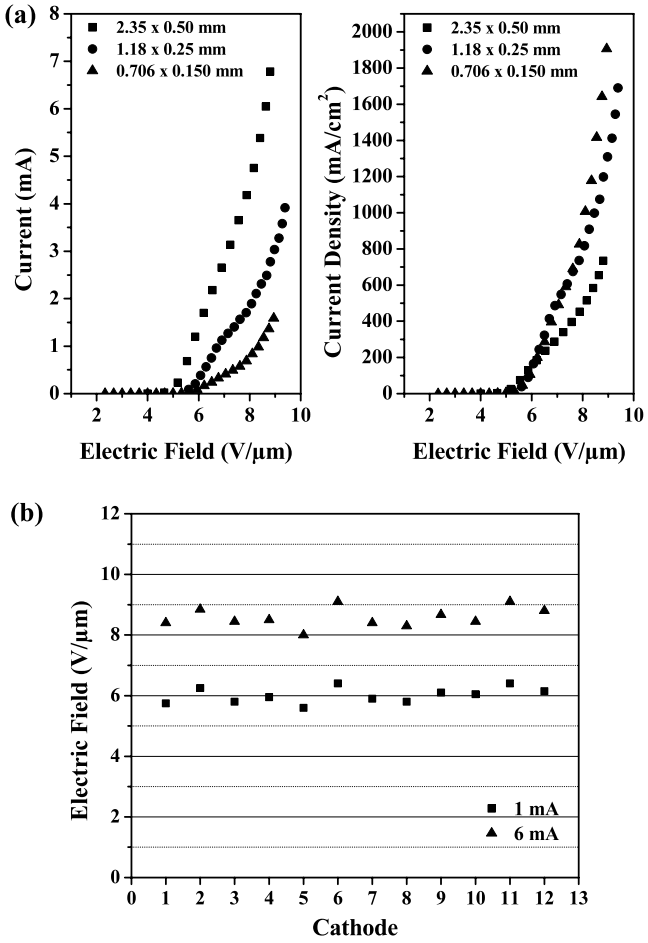

Figure 3. (a) Field emission current versus applied electrical field from 3 cathodes with different dimensions measured in the parallel-plate geometry. The voltage applied to the anode has a square waveform with 10 ms pulse width and 1 Hz repetition rate. The cathode-to-anode distance is 150 μm. The cathode areas are 0.08, 0.23 and 0.92 mm^2, respectively for the 3 cathodes. As shown, over 1500 mA cm^{-2} density was readily achieved. (b) Electrical fields required to reach a peak current of 1 mA (108 mA cm^{-2}) and 6 mA (650 mA cm^{-2}) measured from 12 cathodes (0.50 mm × 2.35 mm elliptical CNT cathode). The waveform of the anode voltage was 10 ms pulse width and 1 Hz and cathode-to-anode spacing of 150 μm was used.

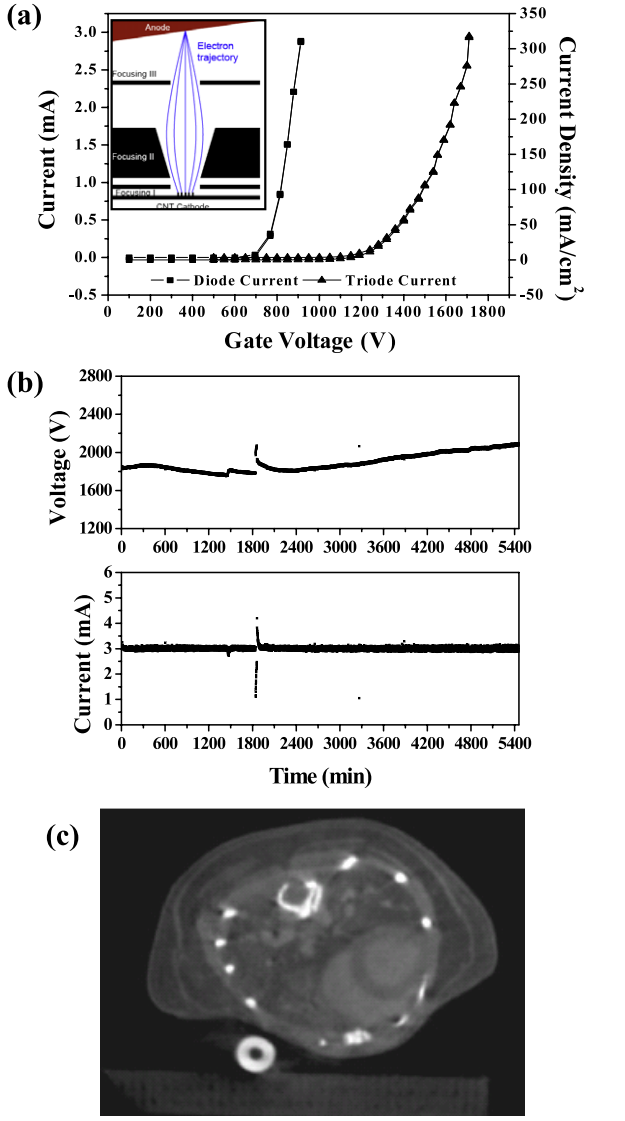

Figure 4. (a) Field emission current as a function of the applied gate voltage from a 0.50 mm × 2.35 mm elliptical CNT cathode at constant anode voltage. For comparison the data from the same cathode measured in the parallel-plate geometry (cathode-to-anode spacing was 150 μm) is also shown. The waveform of the anode voltage was 10 ms pulse width and 1 Hz was used for the diode and triode measurement mode. The difference in the extraction voltage between the two measurements is due to the field non-uniformity from the metal mesh gate frame. (b) Emission lifetime measurement of a 0.50 mm × 2.35 mm CNT cathode at constant current mode in triode geometry. The peak emission current in the pulsed mode was fixed at 3 mA and an averaged peak current of 3.0 ± 0.1 mA was obtained. The distance between gate and CNT cathode was 180 μm. The waveform of the gate voltage was 20 ms pulse width and 1 Hz. An external resistance of 100 kΩ was used. The gate transmission rate (percentage of the current passed through the gate electrode) was 69%. (c) A physiologically gated micro-computed tomography image of anesthetized mouse using the CNT based micro-focused x-ray source. The image was collected using a 20 ms x-ray pulse and 100 μm system resolution.

voltage. As shown in figure 4(b), in the first 30 hours V_g essentially stayed the same, indicating no measurable cathode degradation. After the arcing event occurred at ∼30th hour (indicated by the spikes in the voltage and the current plots) V_g increased gradually over time without affecting emission current. Over the course of 90 h, V_g increased only by 245 V (1.4 V μm^{-1}, or 13%) due to gradual degradation of the CNT cathode. This result shows that the CNT cathode with optimized morphology can deliver the maximum power allowed by the x-ray anode and long-term stability.

To demonstrate the applications of these high performance CNT cathodes, a reconstructed cardiac gated micro-computed tomography (micro-CT) image of an anesthetized free-breathing mouse is shown in figure 4(c). The data was collected using a dynamic micro-CT scanner using a CNT based field emission micro-focus x-ray tube developed at UNC [10]. The high resolution image was collected using a 20 ms x-ray pulse and 100 μm system resolution that is made possible by the high current density achieved from the CNT cathodes fabricated in this study.

Acknowledgments

The works done at UNC were supported by grants from the National Institute of Biomedical Imaging and BioEngineering (NIBIB R33EB004204), the National Cancer Institute (U54CA119343) and Xintek, Inc. Calderón-Colón is supported by a graduate fellowship from NIBIB. Work done at Xintek was partially supported by a grant from NIBIB (R43EB004215).

References

[1] Zhu W 2001 *Vacuum Micro-Electronics* (New York: Wiley)
[2] Choi W B *et al* 1999 *Appl. Phys. Lett.* **75** 3129
[3] Kim H S *et al* 2007 Field emission-back light unit fabricated using carbon nanotube emitter *IMID Digest*
[4] Zhang J *et al* 2005 A stationary scanning x-ray source based on carbon nanotube field emitters *Appl. Phys. Lett.* **86** 184104
[5] Liu Z *et al* 2006 Carbon nanotube based microfocus field emission x-ray source for microcomputed tomography *Appl. Phys. Lett.* **89** 103111
[6] de Jonge N *et al* 2002 High brightness electron beam from a multi-walled carbon nanotube *Nature* **420** 393
[7] Bower C *et al* 2002 On-chip vacuum microtriode using carbon nanotube field emitters *Appl. Phys. Lett.* **80** 3280
[8] Milne W I *et al* 2006 Aligned carbon nanotubes/fibers for applications in vacuum microwave amplifiers *J. Vac. Sci. Technol.* B **24** 345
[9] Cao G *et al* 2009 A dynamic micro-CT scanner based on a carbon nanotube field emission x-ray source *Phys. Med. Biol.* **54** 2323–40
[10] Yang G *et al* 2008 Stationary digital breast tomosynthesis system with a multi-beam field emission x-ray source array *SPIE Proc. Medical Imaging*
[11] Fennimore A M *et al* 2008 Enhancing lifetime of carbon nanotube field emitters through hydrocarbon exposure *Appl. Phys. Lett.* **92** 213108
[12] Scott A W 1993 *Understanding Microwaves* (New York: Wiley)
[13] Zhu W *et al* 1999 Very high current density from carbon nanotube field emitters *Appl. Phys. Lett.* **75** 873–5
[14] Shiffler D *et al* 2004 A high current, large area, carbon nanotube cathode *IEEE Trans. Plasma Sci.* **32** 2152
[15] Wei Y *et al* 2001 Stability of carbon nanotubes under electric field studied by scanning electron microscopy *Appl. Phys. Lett.* **79** 4527–9
[16] Zhang J *et al* 2004 Efficient fabrication of carbon nanotube point electron sources by dielectrophoresis *Adv. Mater.* **16** 1219–22
[17] Wang Z L *et al* 2002 *In situ* imaging of field emission from individual carbon nanotubes and their structural damage *Appl. Phys. Lett.* **80** 856–8
[18] Zhou O *et al* 2002 Materials science of carbon nanotubes: fabrication, integration, and properties of macroscopic structures of carbon nanotubes *Acc. Chem. Res.* **35** 1045–53
[19] Oh S J *et al* 2004 Liquid-phase fabrication of patterned carbon nanotube field emission cathodes *Appl. Phys. Lett.* **87** 3738
[20] Qian C *et al* 2006 Fabrication of small diameter few-walled carbon nanotubes with enhanced field emission property *J. Nanosci. Nanotechnol.* **6** 1346
[21] Oh S and Zhou O 2008 Deposition method for nanostructured materials *US Patent Specification* 7,455,757
[22] Choi W B *et al* 2001 Electrophoresis deposition of carbon nanotubes for triode-type field emission display *Appl. Phys. Lett.* **78** 1547
[23] Flynn M J *et al* 1994 Microfocus x ray sources for 3D microtomography *Nucl. Instrum. Methods* A **353** 312–5